The Sensor Regions of VDAC Are Translocated from within the Membrane to the Surface during the Gating Processes

Jinming Song,* Clare Midson,# Elizabeth Blachly-Dyson,# Michael Forte,# and Marco Colombini*
*Department of Biology, University of Maryland, College Park, Maryland 20742, and #Vollum Institute, Oregon Health Science University, Portland, Oregon 97201 USA

ABSTRACT The motion of the sensor regions in a mitochondrial voltage-gated channel called VDAC were probed by attaching biotin at specific locations and determining its ability to bind to added streptavidin. Site-directed mutagenesis was used to introduce single cysteine residues into *Neurospora crassa* VDAC (naturally lacks cysteine). These were chemically biotinylated and reconstituted into planar phospholipid membranes. In the 19 sites examined, only two types of results were observed upon streptavidin addition: in type 1, channel conductance was reduced, but voltage gating could proceed; in type 2, channels were locked in a closed state. The result at type 1 sites is interpreted as streptavidin binding to sites in static regions close to the channel opening. The binding sterically interferes with ion flow. The result at type 2 sites indicates that these are located on a mobile domain and coincide with the previously identified sensor regions. The findings are consistent with closure resulting from the movement of a domain from within the transmembrane regions to the membrane surface. No single site was accessible to streptavidin from both membrane surfaces, indicating that the motion is limited. From the streptavidin-induced reduction in conductance at type 1 sites, structural information was obtained about the location of these sites.

INTRODUCTION

A variety of intrinsic membrane proteins form channels in membranes that allow specific solutes and usually solvent to cross the membrane. Some of these channel-forming proteins are voltage-gated, in that the transmembrane voltage regulates the nature and permeability of the channel. The opening and closing of the channel reflects conformational changes in the membrane protein that, for the most part, are poorly understood. Voltage-gated channels must possess a voltage sensor that responds to relatively small changes in the transmembrane voltage, and this response is converted, via structural changes in the protein, to permeability changes in the channel.

How voltage gating works, i.e., how proteins change their functional characteristics in response to small changes in voltage, is an unresolved biophysical problem of some interest. In theory, the voltage sensor could be a charged domain that moves along the electric field, or a strong dipole that can reorient with respect to the electric field. In plasma membrane channels, the primary voltage-sensing domain has been identified as the S4 regions of Na, K, and Ca channels. However, other regions are also involved (Seoh et al., 1996). Evidence for motion of the S4 region comes from observations that accessibility to chemical modification at specific sites shifts from one membrane surface to the other (Larsson et al., 1996; Yang et al., 1996). Thus, even in the case of the best known sensor, the dynamic conformational rearrangements associated with gating are still largely undefined. For ectocytic channels (water-soluble proteins (often toxins) that can insert into membranes to form channels) the insertion process is often the voltage-dependent step. For colicin Ia, a substantial fraction of the protein is translocated through the membrane in response to a voltage increase (Slatin et al., 1994). Some of these translocated domains undoubtedly represent the voltage sensor.

We have explored the dynamics of voltage gating in VDAC channels found in the mitochondrial outer membrane (VDAC is also known as mitochondrial porin). VDAC is an abundant protein found in the mitochondria of eukaryotes from all kingdoms (Colombini, 1989). Purified VDAC protein can be introduced into planar phospholipid bilayers, where it forms channels whose properties have been studied extensively (Colombini et al., 1996). The channels are large pores (~3-nm diameter) with a weak selectivity for anions. They are the major pathway through which metabolic intermediates, such as ADP, cross the outer membrane (Benz et al., 1988; Liu and Colombini, 1992; Lee et al., 1994).

Although it forms large pores, VDAC is a small molecule, with a single 30-kDa polypeptide forming each channel. Existing data (Colombini et al., 1996) are consistent with the idea that open channels are formed from a single layer of protein, consisting of one α-helix and 12 β-strands, curved into a cylinder that forms the pore (Figs. 1 and 2). The circled and boxed residues (Fig. 1) must be close to the ion stream, because the use of site-directed mutagenesis to introduce charge changes at these sites in yeast VDAC caused changes in the open channel's selectivity by an amount and in a direction that are related to the engineered

Received for publication 12 December 1997 and in final form 18 February 1998.

Address reprint requests to Dr. Marco Colombini, Department of Biology, University of Maryland, College Park, MD 20742. Tel.: 301-405-6925; Fax: 301-314-9358; E-mail: colombini@zool.umd.edu.

0006-3495/98/06/2926/19 $2.00

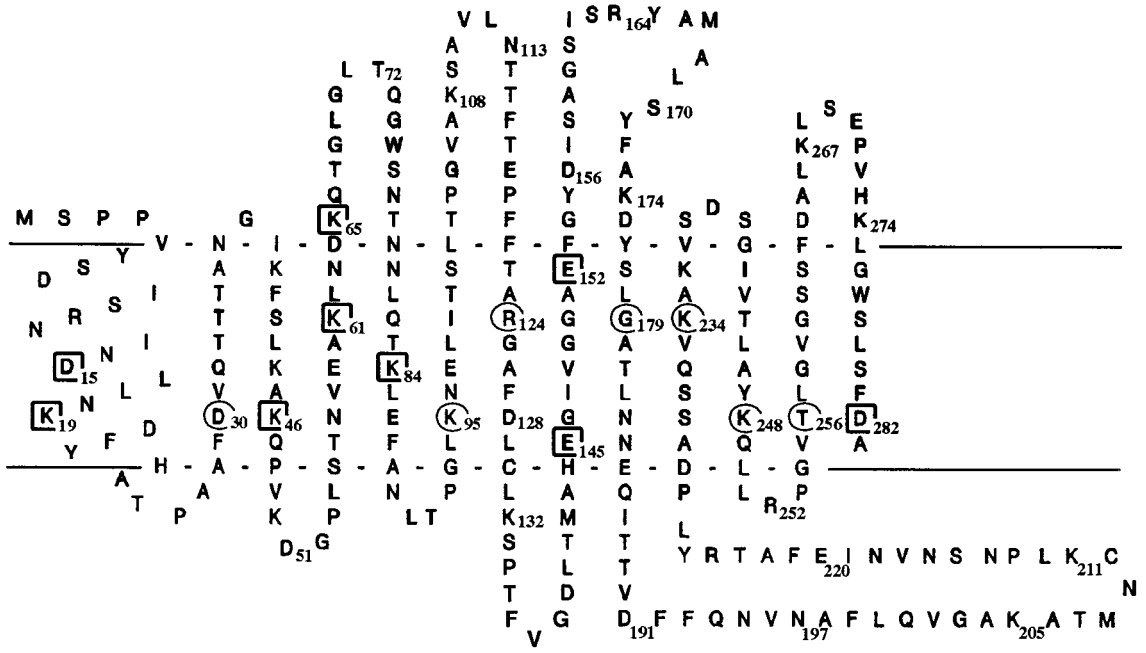

FIGURE 1 The proposed transmembrane folding pattern for VDAC of the yeast *S. cerevisiae*. Previous results are consistent with the VDAC channel being formed by one α-helix (the first 20–25 amino acids) and 12 β-strands forming the walls of the aqueous pore. Site-directed mutations (Blachly-Dyson et al., 1990) were used to change specific amino acid residues (numbered residues) in such a way as to change the net charge at that site. Sites at which charge substitutions changed the open state selectivity are either circled or boxed. Sites whose mutation changed the steepness of the voltage gating process are boxed. The observed changes were of the appropriate sign and magnitude. The lines indicate the boundary of the hydrophobic part of the membrane.

charge change (Blachly-Dyson et al., 1990). This, the hydropathic nature of the protein segments (Peng et al., 1992a), and the location of prolines and tyrosines help support the membrane folding pattern for open channels shown in Fig. 1. Table 1 summarizes the deduced structural features and the supporting evidence.

In planar phospholipid bilayers, VDAC channels are voltage-gated and close in response to applied voltage by two separate gating processes: one at positive transmembrane potentials and one at negative potentials. The "closed" states are not completely closed, but have a 30–40% drop in effective pore diameter (Colombini et al., 1996). Closed VDAC channels have a reversed ion selectivity (i.e., are cation-selective channels) resulting in channels that are very poorly permeable to relevant metabolites such as ATP, succinate, citrate, and phosphate (Bowen et al., 1985; Rostovtseva and Colombini, 1997). The gating processes are symmetrical at the single-channel level in most wild-type VDAC molecules, so the orientation of channel insertion cannot be determined from a channel's electrophysiological properties. Specific site-directed mutations can selectively alter only one of the two gating processes, however (Zizi et al., 1995).

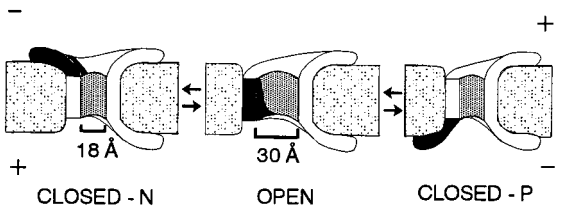

FIGURE 2 The proposed working model for the VDAC gating processes. Longitudinally bisected views of the open state (center) and the closed states achieved at positive (CLOSED-P) and negative (CLOSED-N) potentials. The sensor domain is indicated by the black region. In both gating processes, the sensor domain moves toward the negative side of the membrane.

A number of previous studies have investigated the conformational rearrangements associated with voltage-dependent gating of this molecule. These studies have shown that for both of VDAC's gating processes, decreasing the positive charge on the molecule, either by chemical modification of *Neurospora* VDAC (Doring and Colombini, 1985) or by site-directed mutagenesis at particular locations in yeast VDAC (*boxed residues* in Fig. 1) (Thomas et al., 1993), decreases the voltage dependence of VDAC's gating processes. Conversely, increasing the positive charge in these locations increases the voltage dependence. This is consistent with a positively charged domain of the protein moving through the transmembrane electric field during each gating process. Most of the sites at which charge changes affect the steepness of the voltage dependence are located in the amino-terminal 84 residues of the protein, implicating this region as a domain that moves during gating. A mutation-induced charge change at at least one site (residue 46) affects both gating processes, indicating that the domains that move during the two gating processes overlap each other.

TABLE 1 Summary of structural information for VDAC from *S. cerevisiae*

Region	Structure	Membrane spanning	Evidence*	On sensor	Evidence#
1–23	α	Yes	S_o(15,19)	Yes	S_c(15,19)V(15,19)
24–27	Turn	No			
28–37	β	Yes	S_o(30)	No	S_c(30)V(30)
38	Turn	No			
39–48	β	Yes	S_o(46)	Yes	S_c(46)V(46)
49–54	Turn	No	S_o(51)	No	V(51)
55–65	β	Yes	S_o(61,65)	Yes	S_c(61,65)V(61,65)
66–78	Surface	No	S_o(72)		
79–88	β	Yes	S_o(84)	Yes	S_c(84)V(84)
89–92	Turn	No			
93–102	β	Yes	S_o(95)	No	S_c(95)V(95)
103–120	Surface	No	S_o(108,113)		
121–130	β	Yes	S_o(124,128)	No	S_c(124,128)V(124)
131–143	Surface	No	S_o(132)	No	V(132)
144–153	β	Yes	S_o(152)	Yes	S_c(152)V(145,152)
154–175	Surface	No	S_o(156,164,170,174)	No	V(156)
176–185	β	Yes	S_o(179)	No	S_c(179)
186–227	Surface	No	S_o(191,197,205,211,220)	No	V(205,211)
228–237	β	Yes	S_o(234)	No	V(234)
238–240	Turn	No			
241–250	β	Yes	S_o(248)	No	V(248)
251–253	Turn	No	S_o(252)	No	V(252)
254–263	β	Yes	S_o(256)		
264–274	Surface	No	S_o(267,274)	No	V(267)
275–283	β	Yes	S_o(282)	Yes	S_c(282)V(282)

The region refers to the numerical location in the primary sequence starting with the N-terminus. The methionine is considered number 1, even though it is probably not present in the mature protein. The structures are α-helix, β-strand, a short turn, or a surface domain of unknown structure. Under "evidence," S_o, S_c, and V are effects of mutations, at the indicated positions, on the selectivity of the open state, selectivity of the closed state, and steepness of the voltage dependence, respectively.

*Blachly-Dyson et al. (1990) and Peng et al. (1992).

#Peng et al. (1992), Thomas et al. (1993), and Zizi et al. (1995).

A second line of evidence supports the identification of these same domains as the sensor regions in VDAC. Whereas charge changes introduced at the boxed residues influenced the selectivity of the open state, these same mutations have a smaller effect than expected or no effect on the selectivity of the "closed" state (Peng et al., 1992b). This indicates that in the transition from the open to the closed state, these sites had moved away from the ion stream and thus likely through the field to the membrane surface. Table 1 indicates the regions presumed to form the sensor domains.

These studies and others are consistent with a mechanism for voltage gating in VDAC, whereby a domain with net positive charge forms part of the wall lining the open channel that is driven out of the channel by an electric field of either direction, resulting in a closed state with reduced pore diameter and inverted ion selectivity (Fig. 2). To directly test this idea at the protein level, we used a technique developed by Slatin et al. (1994) in the analysis of the conformational changes associated with channel formation by the colicin Ia molecule. Cysteine residues were introduced at sites within and outside the proposed sensor regions, using site-directed mutagenesis. Each VDAC protein containing a single cysteine residue was then treated with a reagent that covalently attached a biotin molecule to the cysteine residue. The biotinylated VDAC proteins were inserted into planar phospholipid bilayers, and their channel properties were observed before and after streptavidin was added to the bath on one or both sides of the bilayer. If the biotin moiety on the VDAC protein is exposed at the surface of the membrane, streptavidin should bind tightly to the biotin. Streptavidin binding should interfere with subsequent voltage-driven conformational changes, because streptavidin is a large water-soluble protein that will prevent movement into or through the membrane. Thus, if the biotinylated residue is located in the voltage sensor, the binding of streptavidin should prevent gating by holding the sensor on one side of the membrane. If the biotinylated residue is in a nonmobile portion of the molecule, gating might proceed normally. The results presented here show that single biotinylated residues in the VDAC molecule respond to added streptavidin in one of these two ways. For some biotinylated sites, the addition of streptavidin reduced the channel's conductivity but allowed gating to occur. In others, streptavidin binding trapped the channel in a closed state. These results demonstrate directly at the protein level that voltage gating in this protein is associated with the movement of voltage-sensing residues from within the membrane to the membrane surface.

MATERIALS AND METHODS

Site-directed mutagenesis and expression of mutant proteins

Single cysteine substitutions were engineered into the cDNA encoding *Neurospora crassa* VDAC because this protein lacks cysteine residues. Sites were chosen on the basis of existing models of the structure of the open channel and the conformational transitions that accompany closing (Colombini et al., 1996). In addition, a sequence encoding a GlyGlyCys extension was attached to the C-terminus. To construct this C-terminal extension, the coding region of the *N. crassa* VDAC cDNA was amplified with an oligonucleotide at the 5′ end of the coding region that included an *Nco*I restriction site, and a 3′ oligonucleotide containing codons encoding GlyGlyCys, Stop, and a *Nsi*I site (GGAGATGCATTAACAACCACCA-GACTCGAAGGTGAAGC).

The resulting amplification product was digested with *Nco*I and *Nsi*I, and inserted between the yeast YVDAC1 5′ and 3′ noncoding regions for expression in yeast. All of the single mutants are labeled with the letter-number-letter notation. The number is the location of the amino acid in the primary sequence starting at the amino terminus, and the leading and tailing letters represent the amino acid in the wild-type and mutant, respectively. The numbering includes the N-terminal methionine, which is probably removed in the mature protein.

The plasmid encoding *N. crassa* VDAC was subjected to site-directed mutagenesis by standard protocols and introduced into a yeast strain, M22-2, that lacks the chromosomal copy of the gene that codes for YVDAC1, the only yeast gene product that forms classical VDAC channels (Blachly-Dyson et al., 1997). Expression of wild-type and mutant cDNAs in yeast was mediated by sequences representing the YVDAC1 promoter (Blachly-Dyson et al., 1997). VDAC proteins were purified from the mitochondrial outer membranes by the method described by Blachly-Dyson et al. (1990).

Biotinylation of mutant VDAC proteins

Attachment of biotin molecules to cysteine residues was performed using the method described by Qiu et al. (1994). The biotinylating reagent, 3-(-*N*-maleimidylpropionyl) biocytin (Molecular Probes, Eugene, OR), includes a 1.6-nm arm (if fully extended and measured from the carbonyl group of the biotin moiety) that allows the biotin to penetrate the deep cleft in streptavidin. This cleft has been measured to be 0.9 nm deep (from the carbonyl of the bound biotin moiety), and therefore the once the biotin portion of the biotinylated group has bound to the site on streptavidin, the maximum distance between the surface of the streptavidin and the sulfur of the cysteine residue to which the streptavidin is attached is 0.7 nm. Because of the rigidity of the amide linkage and the ring system on this arm, the lateral displacement of the two proteins is more limited. We estimate a 0.5-nm freedom of displacement on either side of the point of binding.

Typically, 1 ml of purified VDAC in 15% dimethyl sulfoxide, 2.5% Triton X-100, 50 mM KCl, 1 mM EDTA, 10 mM Tris-Cl (pH 7.0), containing ~20 μg of protein, was obtained from one preparation. Immediately after isolation and purification (to minimize cysteine oxidation), 600 μl of the purified VDAC solution was biotinylated by adding 60 μl of 2 M sodium phosphate, 100 mM EDTA (pH 7.0), and 300 μl of 3-(-*N*-maleimidylpropionyl) biocytin (3 mg/ml dissolved in 3:2 dimethylsulfoxide and dimethylformamide). The reaction was carried out at room temperature for 1 h and was stopped by adding 16 μl β-mercaptoethanol (14.2 M). Excess biotinylating reagent was removed by dialysis against 1 liter of buffer (1% Triton X-100, 50 mM KCl, 10 mM HEPES, 1 mM EDTA, pH adjusted to 7.0 with KOH) for 24 h at 4°C.

Estimation of the extent of biotin modification

The extent of biotin modification of each mutant protein was estimated by two independent techniques. First, purified proteins, before or after the biotinylation reaction, were precipitated from 100 μl of sample by the addition of 1/3 volume methanol and 1/3 volume 50% trichloroacetic acid and incubated for 15 min at 4°C. Precipitated proteins were collected by centrifugation, and pellets were washed with acetone and air dried. Samples were resuspended in 10 μl (biotinylated) or 30 μl (unbiotinylated) 1% sodium dodecyl sulfate (SDS) in 50 mM Tris (pH 7.5) and diluted to 0.1% SDS with 50 mM Tris (pH 7.5). For electrophoresis, 6 μg of streptavidin (Pierce, Rockford, IL) was incubated with 60-μl aliquots of protein for 30 min at room temperature, then mixed with 30 μl low-SDS (0.4%) loading buffer lacking reducing agent. Ten microliters of each sample was then run on 10% sodium dodecyl sulfate–polyacrylamide gel electrophoresis (SDS-PAGE) minigels and electroblotted onto nitrocellulose, and blots were incubated with an antibody generated to a peptide representing the C-terminus of *N. crassa* VDAC (W937; Stanley et al., 1995). Antibody binding was detected by chemiluminescence after a 30-min exposure of a Molecular Imager System (Biorad) chemiluminescent sensitive screen. Digitized bands were analyzed for relative densities with the Molecular Analyst Program.

When purified, biotin-modified VDAC was run on SDS-PAGE gels in the absence of streptavidin under the above conditions. A small fraction of the total immunoreactive protein has a molecular weight roughly double that of the VDAC monomer and approximately that expected for VDAC-streptavidin complexes. This band likely represents VDAC dimers that are known to form in preparations of purified protein (Mannella and Colombini, 1984) and which apparently are resistant to dissociation under these low-SDS conditions. To correct for the extent of biotinylation in the presence of this dimer, dimers were assumed to represent populations of VDAC molecules that were biotinylated to the same extent as monomers. Thus the percentage of biotinylation is given by

$$\% \text{ biotinylation} = 100(100 - B - D)/(100 - D)$$

where B is the percentage of the total intensity in the streptavidin lane that is located at ~30 kDa, and D is the percentage of dimers in the lane without streptavidin.

A second, functional estimate of the extent of biotin modification was also used. The percentage of conductance decrease upon the addition of streptavidin to single channels was compared to the decrease observed in membranes containing multiple channels (typically 25–50) after streptavidin addition. By dividing the latter by the former, the percentage of channels affected by streptavidin was estimated. The results obtained from different multiple-channel experiments for each mutant were averaged.

Electrophysiological studies

VDAC proteins were reconstituted into planar phospholipid bilayers (soybean phospholipids) by adding an appropriate amount of detergent-solubilized samples to the *cis* side of the chamber. The membranes were made as previously described (Colombini, 1987). All experiments were performed in the presence of buffered solutions (1.0 M KCl, 1 mM $CaCl_2$, 5 mM 2-(*N*-morpholino)ethanesulfonic acid (pH 5.8)) on both sides of the membrane. Calomel electrodes were used to interface with the solutions via the built-in saturated KCl bridge. The experiments were performed under voltage clamp conditions. All of the results were corrected for any electrode asymmetry. The current was recorded on a Kipp and Zonen chart recorder with a response time of 0.3 s, full scale deflection. In this paper, the *cis* side refers to the side to which the VDAC sample was added. The sign of the applied voltage always refers to the *cis* side (*trans* is virtual ground).

After insertion, channel properties were characterized by assessing single-channel conductance and voltage dependence. The biotinylated channels often had a conductance that was somewhat reduced, by as much as 20%. However, like the wild-type, all of the mutant channels showed voltage-dependent gating at both positive and negative potentials, and the gating occurred at normal rates. Therefore, the channels were judged to be suitable for further experimentation with streptavidin. Generally, 20 μl of the streptavidin stock solution (2 mg/ml) was added to the 5-ml buffered solution on one side or both sides of the membrane, when the channels

were held open or in one of two closed states by means of the applied electrical potential, as dictated by the experiment. Thus there was a choice of one of six ways of beginning the experiment.

Calculation of the degree of occlusion by streptavidin binding

A theoretical calculation was undertaken to obtain structural information from the degree of reduction in conductance resulting from streptavidin binding to type 1 mutants. This calculation allowed us to find a relationship between the average amount of unobstructed area of the pore and the distance from the site of streptavidin attachment on VDAC and the rim of the pore. It was assumed that streptavidin could take all possible orientations. The opening of the channel was taken as a circle 3 nm in diameter. The streptavidin footprint (effective region of surface contact that could block ion flow) was taken from the literature by comparing the crystal structure in the protein data bank (Weber et al., 1989) to the structure and orientation of streptavidin on biotinylated phospholipid monolayers (Avila-Sakar and Chiu, 1996). Fig. 12 shows this rectangular footprint with the two binding sites that would face the surface of the membrane. Because this structure has twofold rotational symmetry, we need consider only one of the binding sites. The site is connected via a molecular linker to the sulfur of the cysteine, allowing an estimated 0.5-nm lateral motion. The location of the streptavidin footprint in relation to the pore opening is defined by three parameters: t, α, and δ. t is the distance from the center of the pore to the cysteine sulfur. α is the angle formed by the intersection of the two lines connecting the cysteine sulfur either to the center of the pore or to the binding site on streptavidin. δ is the angle formed by the line connecting the binding site on streptavidin to the cysteine sulfur and that forming a perpendicular to one edge of the streptavidin footprint (Fig. 12). The average unobstructed area was calculated for values of t ranging from 1.5 nm to the point where no obstruction occurred at 0.1-nm intervals. For each value of t, 10,000 random values of α and δ were used to calculate the average unobstructed area. The length of the molecular connection was also allowed to vary randomly between 0 and 0.5 nm.

The fraction of the open-state conductance that remained after streptavidin binding to each type 1 site was compared to the calculated fraction of unobstructed area from the above calculations to determine the distance from the cysteine sulfur to the rim of the pore. We assumed that conductance was proportional to unobstructed area.

RESULTS AND DISCUSSION

By the introduction of a cysteine residue into a VDAC channel, one can introduce a site that can be specifically biotinylated, and then its location can be probed with streptavidin. A change in accessibility to streptavidin resulting from a voltage-induced conformational change in VDAC would provide direct evidence for motion of the site. Unlike small-molecular-weight reagents that might penetrate into protein crevices, cross the membrane through the pore, or cross by solubility/diffusion through the lipid membrane, streptavidin is large (60 kDa) and highly water soluble, and thus cannot penetrate to any meaningful extent. The localization is precise to one amino acid residue, and the penetration into the membrane is limited to 0.7 nm by the length of the molecular linker connecting streptavidin to the cysteine.

VDAC from *N. crassa* lacks cysteine residues and therefore constitutes a logical starting point for the introduction of individual cysteine mutations in this protein. cDNAs expressing mutant forms of this protein containing single cysteine substitutions were expressed in a yeast strain with its major endogenous VDAC gene deleted. The cysteine residue on VDAC channels purified from these cells was biotinylated before incorporation of the channels into planar phospholipid membranes. The conductivity and gating properties of these channels were observed in membranes containing single or multiple channels, and any changes in these properties after the addition of streptavidin were noted. The side of the membrane to which VDAC was added is referred to as the *cis* side, and the opposite side as the *trans* side. The sign of the transmembrane potential was taken to be the sign of the potential on the *cis* side of the membrane. In all cases, assignment of individual sites to one of the two general categories described below was confirmed by analysis of membranes containing both single and multiple channels.

Control experiments

Control experiments were run to confirm that streptavidin addition would affect VDAC channels only if a cysteine had been introduced into the channel and that cysteine had been biotinylated. In this way, direct effects of streptavidin on the channel and biotinylation at sites other than the cysteine could be ruled out.

When unbiotinylated VDAC channels containing cysteine at a single position were exposed to streptavidin on either side of the membrane, no effect was observed. Fig. 3 *A* shows results collected on a multichannel membrane containing unbiotinylated VDAC channels in which T at position 53 had been replaced with C (T53C). The channels were open at low potentials (+9 mV or −11 mV) and slowly closed at elevated positive or negative potentials (+59 mV or −61 mV) both before and after streptavidin addition to either side of the membrane. This is normal behavior for a VDAC channel. In addition, the channels open virtually instantaneously, and this is expected, because VDAC channels generally open in a millisecond or less. Likewise, when wild-type VDAC channels devoid of cysteine residues were treated with the biotinylating reagent and then inserted into membranes, addition of streptavidin to either side of the membrane had no effect. Fig. 3 *B* shows an experiment in which streptavidin was added to a single wild-type VDAC channel that had been treated with biotinylating reagent. The channel was open at a low potential and closed at elevated positive and negative potentials. This voltage-dependent behavior was the same before and after streptavidin addition. Thus the deviations from normal channel activity noted below specifically depend on the binding of individual biotin-modified sites to added streptavidin.

Type 1 mutants: streptavidin binding does not stop the gating process, but lowers the conductivity

When streptavidin was added to channels biotinylated at a single introduced cysteine residue, two types of effects were

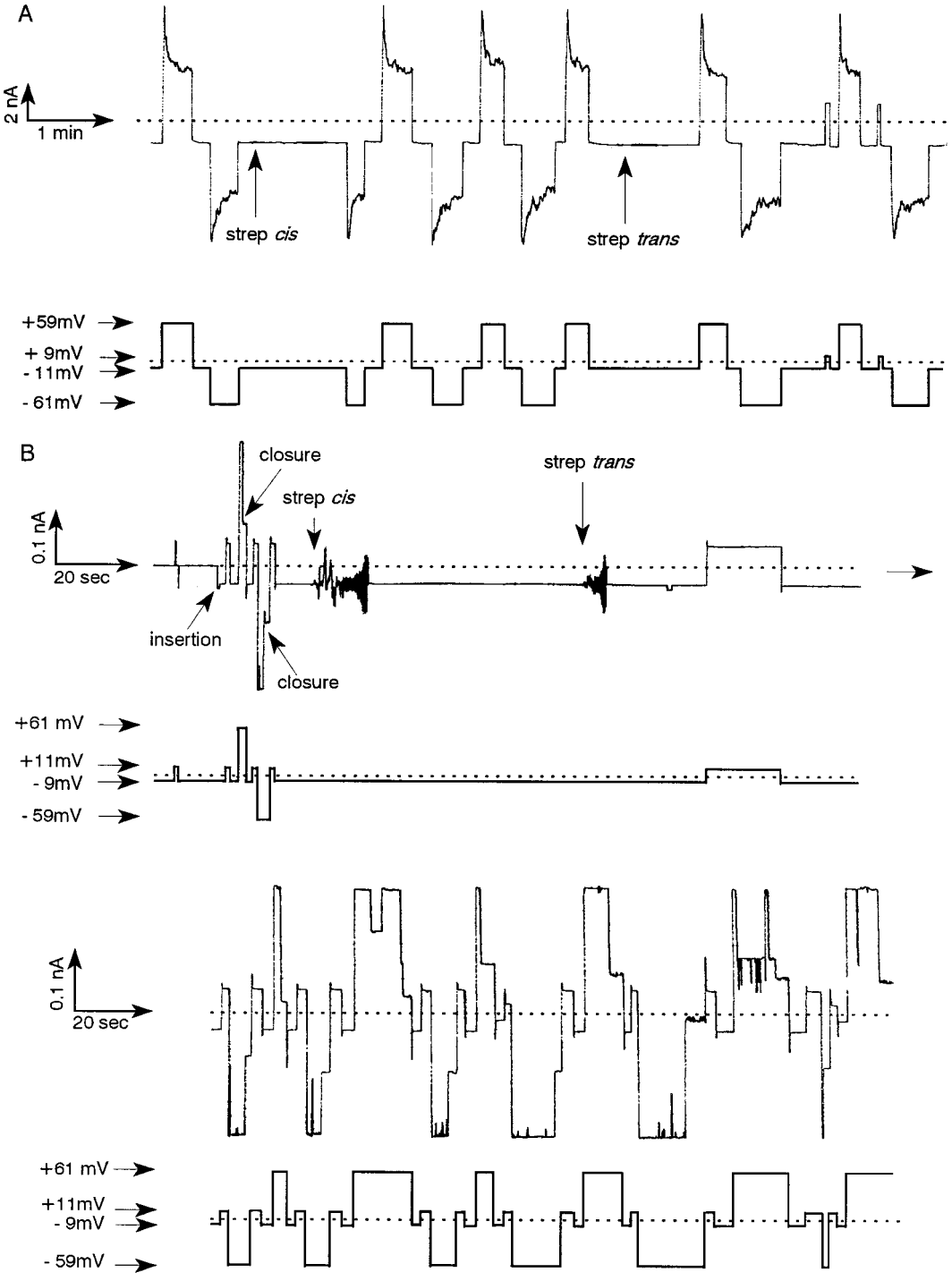

FIGURE 3 Lack of effect of streptavidin on unbiotinylated cysteine-containing channels or wild-type channels treated with the biotinylation procedure. Channels were inserted in a planar membrane under standard conditions (see Materials and Methods). In *A* the membrane contained multiple *N. crassa* VDAC channels containing the mutation T53C. In *B* a single wild-type *N. crassa* VDAC channel was studied. In each panel, part of the current record is shown just above its corresponding voltage trace. In *B* the current and voltage traces continue without temporal gaps from the upper portion to the lower portion. The dotted lines are the zero current or voltage levels. Streptavidin was added to each side of the membrane where indicated. The single-channel insertion and some closing events are indicated. The sign of the applied voltage refers to the *cis* side of the membrane, the side to which the VDAC protein was added.

observed. In one group of mutants (type 1), streptavidin addition reduced the channel conductance, but allowed voltage gating to proceed. In a second group (type 2), streptavidin locked the channels in a closed state. The mutation D264C is an example of a type 1 mutation. When biotinylated D264C channels were treated with streptavidin on the

cis side of the membrane (the side to which the VDAC protein had been added), the conductance of the channel dropped. This is illustrated with a single channel in Fig. 4 *A*. Twenty seconds after streptavidin addition, a discrete drop in conductance occurred (labeled "strep binding"). This is undoubtedly the time point at which streptavidin bound to the biotinylated site, because after such an event, the properties of these channels change abruptly. The conductance drop was not a closing event, because the channel could be closed by applying a high positive potential (+61 mV). Thus the binding of streptavidin was probably interfering with ion flow and not causing channel closure. Voltage-dependent closure at negative potentials occurs, but is now less frequent. The channel had to be held at −59 mV for an

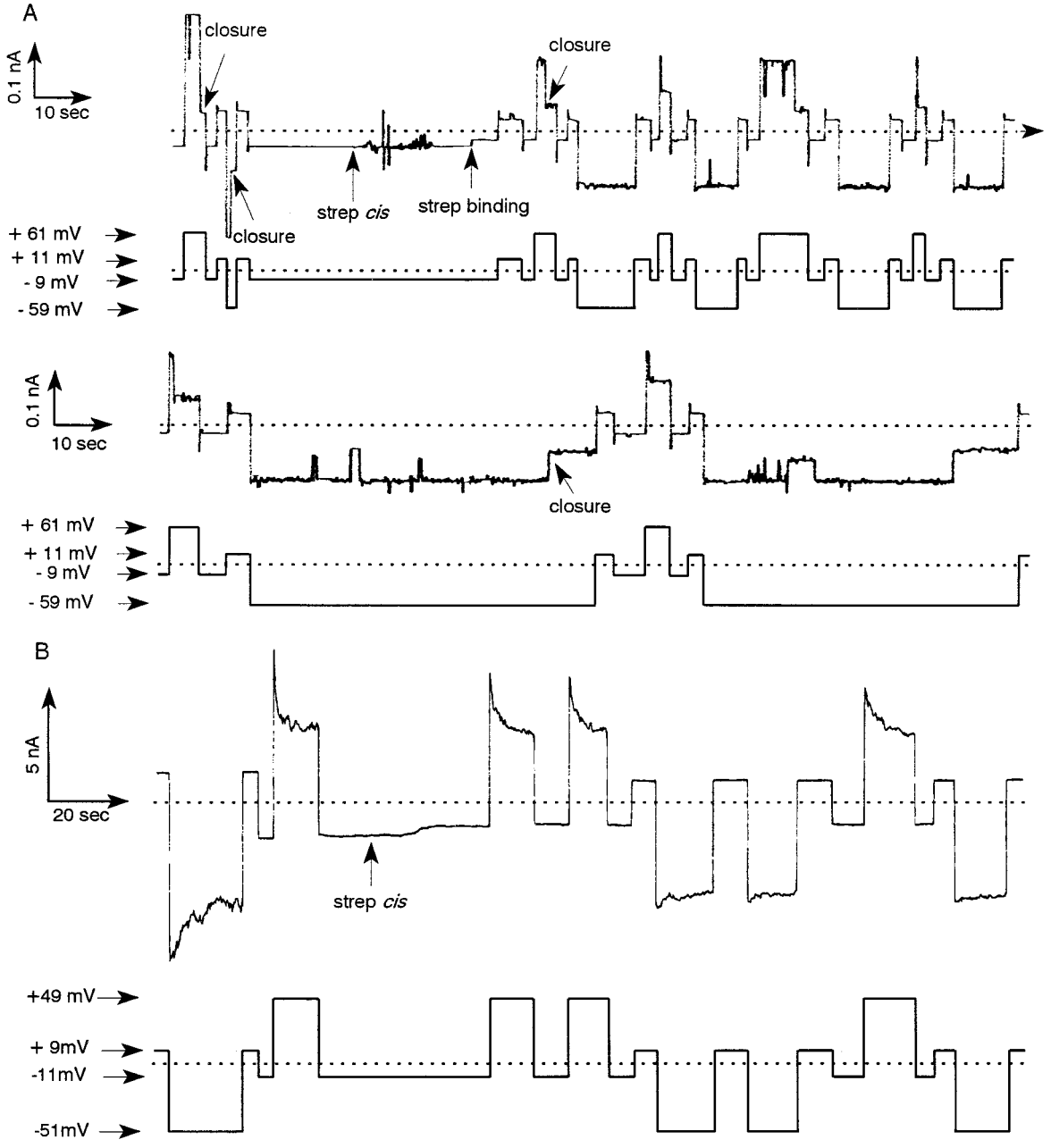

FIGURE 4 Streptavidin binding to VDAC channels biotinylated at position 264 reduced the conductance, but did not stop the gating process. At the point indicated, streptavidin was added to a membrane containing a single (*A*) or multiple (*B*) D264C VDAC channels. In *A* the current trace and corresponding voltage trace (*below*) are continuous from the upper to the lower record. The point of streptavidin binding and selected closures are indicated.

extended period to observe the closing events (*lower trace*). There is a reduced probability of finding the channel in the closed conformation, and therefore the closed state is less favored.

These observations are understandable if we picture the large streptavidin molecule being tethered to a site close to the mouth of the channel (Fig. 5). Its presence would introduce resistance to ion flow by acting as an obstacle. The selective interference of gating in response to negative potentials can be understood in terms of the current model (Fig. 5) for voltage gating in VDAC. A negative potential on the streptavidin side would pull the positively charged sensor to the surface, and the presence of the tethered streptavidin on that side would be expected to interfere, sterically, with the motion. This interference with closure when the streptavidin side was made negative was seen in all type 1 mutations. No effect on the rate of reopening was detected.

In multichannel membranes (Fig. 4 *B*), biotinylated D264C channels exhibited a drop in conductance after the addition of streptavidin to the *cis* side of the membrane. No effect was observed if streptavidin had been added to the *trans* side (not shown), indicating that streptavidin only acts from one side, and that all the channels were oriented in the same direction. Again, at elevated positive potentials (+49 mV), these lower-conducting channels showed normal voltage gating properties, whereas at negative potentials (−51 mV) there was little closure, because of a lower probability of entering the closed states. Note that the drop in conductance in this pool of channels was very similar to that observed for the single channel in Fig. 4 *A*.

Biotinylation of single cysteine substitutions at five other sites produced results similar to those presented for D264C. These sites (K92, K112, T135, D156, and R240; Table 2) were located in regions previously identified as being outside the mobile domain. A sixth site (N38C) was also identified as type 1, but, in this case, streptavidin acted from both sides when multichannel membranes were examined. Streptavidin seemed to affect only subsets of the channel population, indicating that channels had inserted in both directions (see last section for information on insertion direction). This is borne out in single-channel experiments. Modified N38C channels were affected by streptavidin only on one side of the membrane, although the effective side varied from membrane to membrane. In these single-channel experiments, as with the mutants that always were affected on one side, N38C channels gated normally when the streptavidin side was made positive, but gating was interfered with when the side of streptavidin addition was made negative. As is the case with the other type 1 sites, a negative potential on the streptavidin side would drive the sensor toward the bound streptavidin.

The fact that all of these sites at very different locations in the molecule show the same result is strong evidence for our interpretation of the way streptavidin interferes with channel function. Hypotheses based on an indirect action would have to propose a series of fortuitous coincidences.

TABLE 2 The effective side of streptavidin for type I and type II mutants in the experiments with membrane containing multiple channels (25–50)

Type	Mutants	*Cis*	*Trans*
1	N38C	+	+
	K92C	+	−
	K112C	+	−
	T135C	+	−
	D156C	+	−
	S211C	+	−
	R240C	+	−
	D264C	+	−
2	S7C	+	+
	S12C	−	+
	H23C	+	−
	T53C	+	−
	E58C	+	−
	T69C	+	+
	A79C	+	−
	T183C	+	−
	S190C	+	−
	E282C	−	+
	C-terminal GGC extension	−	+

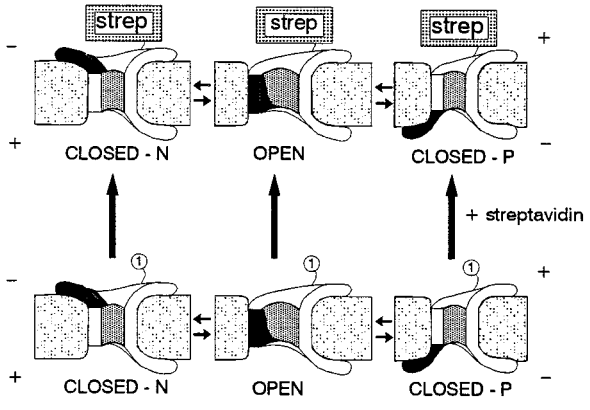

FIGURE 5 Mechanistic interpretation of the type 1 streptavidin effect. Type 1 sites are proposed to be on a static region of the channel. Streptavidin can therefore bind to biotinylated type 1 sites in any of the three voltage-dependent conformations. After streptavidin binding, voltage gating still occurs.

Type 2 mutants: streptavidin binding blocks voltage gating and locks the channel in a low-conducting state

The binding of streptavidin to a domain that must move into and out of the membrane during the gating process might be expected to block this motion and, as a consequence, the conformational change. Fig. 6 *A* shows the effect of streptavidin addition to a membrane containing a single biotinylated T53C channel. Before streptavidin addition, the channel is open at ±10 mV, and it closes after steps to ±50 mV (i.e., normal behavior). As with most type 1 mutations, the

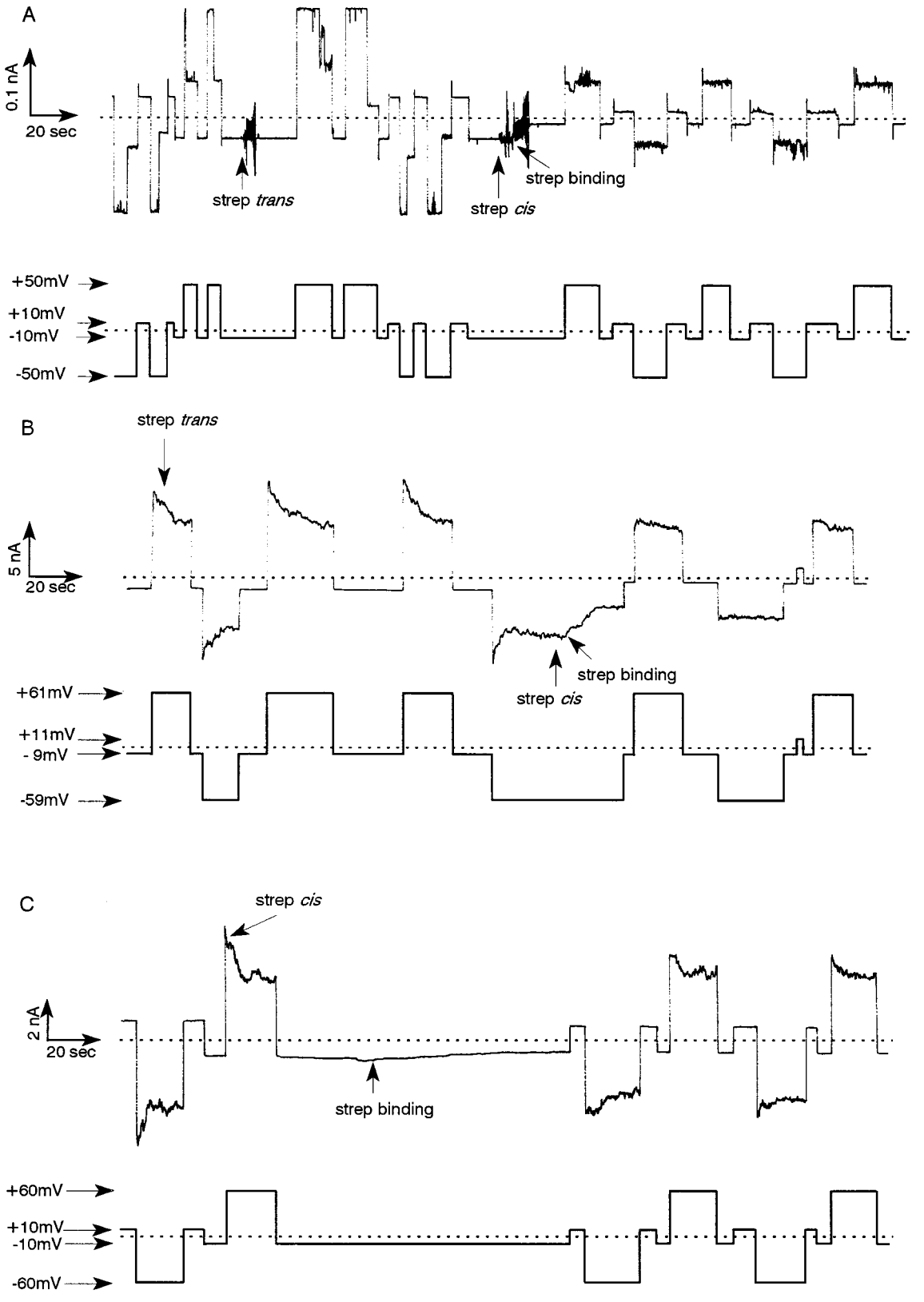

FIGURE 6 Streptavidin traps VDAC channels biotinylated at position 53 in the negative closed state. (*A*) Streptavidin was added while a single biotinylated T53C VDAC channel was in the open state under the influence of a weak negative potential (−10 mV). The conductance drop after streptavidin addition to the *cis* side is interpreted as streptavidin binding and is so labeled. The noise recorded at the points of streptavidin addition was due to mechanical stirring. (*B*) Streptavidin was added to the *cis* side of a membrane containing many biotinylated T53C VDAC channels after the channels had been closed by the application of −59 mV. (*C*) Streptavidin was added to the *cis* side of a multichannel membrane as in *B*, but here the channels were first closed by applying +60 mV. In *B* and *C*, the label "strep binding" indicates the point when the conductance begins to decline.

addition of streptavidin to the *trans* side of the membrane has no effect on this behavior. However, after *cis* addition of streptavidin to the open channel, the channel's conductance dropped dramatically, to a level similar to that of a closed channel. In this experiment, the effect was so rapid that it occurred during the stirring period, in which mechanical agitation causes noise in the record. The fact that the channel remained in this low-conductance state, regardless of changes in applied potential, is consistent with the streptavidin binding having immobilized the voltage sensor in the closed conformation.

Similar results were observed in a multichannel membrane containing biotinylated T53C channels (Fig. 6 *B*). The addition of streptavidin to the *trans* side of the membrane had no effect, showing that all channels are oriented in the same direction. More importantly, there is no structural state in which the biotinylated group was accessible to streptavidin on the *trans* side, because voltage was used to drive the channel into the three basic conformations: open, closed-N (the negative closed state), and closed-P (the positive closed state). In this example, the channels had been closed with a negative potential (−59 mV) before the *cis* addition of streptavidin. Note the immediate additional decline in current. Subsequent attempts to close channels were ineffective, presumably because most of the channels were locked in a closed state.

The channels could only be trapped closed when they were in the correct closed state. If the channels were closed with a positive potential (yielding closed-P), rather than a negative potential (yielding closed-N), there was no sign of streptavidin binding (Fig. 6 *C*). When the channels were reopened by reducing the potential from +60 to −10 mV, at first the current flow was identical to that recorded just previously. However, 40 s later, the first signs of a conductance decline began. From single-channel observations (as in Fig. 6 *A*), this decline is likely the result of channel closure. Its slow onset is consistent with the open channels flickering to the negative closed state and then being trapped by the streptavidin. The onset of the effect is certainly much slower than that in Fig. 6 *B*. After the conductance decline, voltage gating in response to elevated potentials was reduced. The significant amount of residual voltage-gated closure in this experiment is undoubtedly due to unbiotinylated channels in the membrane. Despite the presence of excess streptavidin, no further reaction occurred.

In addition to T53C, biotinylated VDAC channels with cysteine substitutions at S7, H23, E58, A79, T183, and S190 all showed the characteristic type 2 effect after streptavidin addition to the *cis* side (Table 2). VDAC with cysteine substitutions at positions S12 and E282, and a C-terminal extension (C-terminal GGC) were also found to be type 2 sites, but were accessible from the *trans* side of the membrane.

Fig. 7 shows tracings from experiments with E282C. In Fig. 7 *A*, a multichannel membrane containing biotinylated E282C channels was first tested for gating at positive and negative potentials, and then streptavidin was added to the *cis* side. No change was observed in gating or conductivity. Streptavidin was then added to the *trans* side, while the channels were exposed to a −50 mV transmembrane potential. Close observation reveals that after the voltage was changed to +10 mV, channels were reopened and subsequently the conductance dropped. This is an observation analogous to that illustrated in Fig. 6 *C*. However, here position 282 was not accessible to streptavidin (present in both compartments) when VDAC was held in the closed-N state. Because we do not know the absolute orientation of the channels, we do not know if we are dealing with the same state.

The relatively low percentage of biotinylation at position 282 consistently resulted in a population of channels that failed to be affected by streptavidin. Nevertheless, the percentage drop in conductance after the application of an elevated potential (Fig. 7 *A*) was greatly reduced after streptavidin addition. This is consistent with channels being trapped in a closed state but, in isolation, this could easily be interpreted in different ways.

A single-channel experiment for position 282 (Fig. 7 *B*) allows for a definitive assignment of this site as a type 2 mutation. Here again, *cis* addition of streptavidin is ineffective, but *trans* addition while the channel is held in the positive closed state results in an inability of the channel to reopen. As the voltage was changed to try to move the channel to a different conducting state, some transitions were visible (Fig. 7 *B*). These were infrequent and attributable to "subclosed states" (states of lower conductance than the normal closed state) that are easily observed with normal VDAC channels. Bona fide openings were never observed, indicating that the channel binds to streptavidin while in closed-P. In some single-channel experiments, streptavidin was ineffective, showing that some of the channels were not biotinylated.

The ability of biotinylated channels containing type 2 mutations to respond to streptavidin while in the open state is more clearly illustrated in Fig. 7 *C*, where the membrane contains only a few biotinylated channels. Note that the closing steps are distinct and discrete and that the overall process is slow. A low voltage that favors the open state (−10 mV) was applied. However, the channels probably flicker to the positive closed state and are trapped there by the streptavidin. Toward the end of the trace, a new channel inserted and was induced to close by streptavidin on the *trans* side. This is not observed when streptavidin is present on the *cis* side, because it binds the biotinylated VDAC and prevents further channel insertion.

In all type 2 sites, streptavidin could trap the channel closed only from one side of the membrane, and only if the channels were held in the appropriate conformation. If streptavidin were added when the channel was closed with a positive potential on the streptavidin side, no effects would be seen until the potential was reduced, allowing the channels to reopen. Clearly, this result can occur in multichannel membranes only if all of the channels are oriented in the same direction. More importantly, it shows that no site examined so far is accessible to streptavidin from both

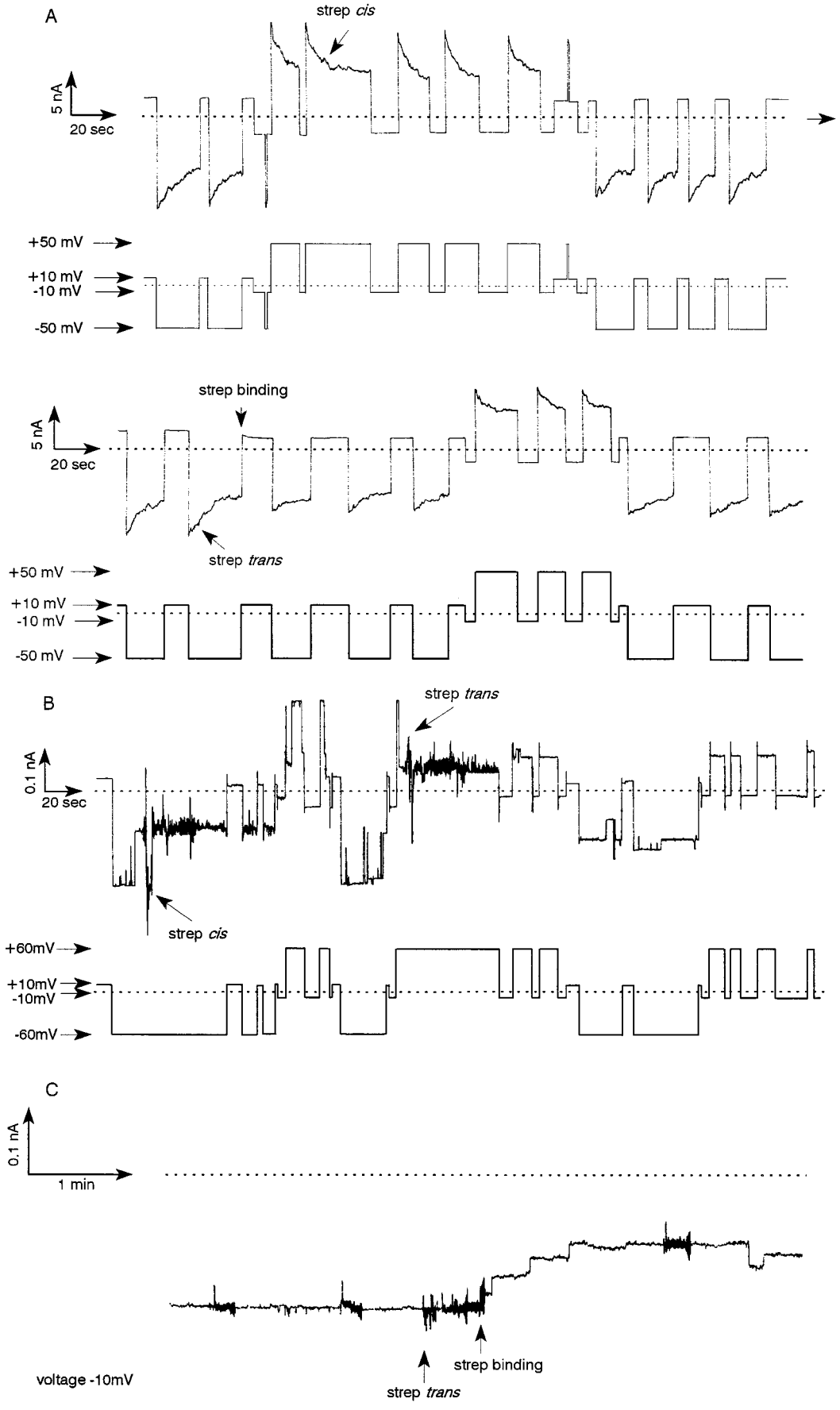
A
strep *cis*
5 nA
20 sec
+50 mV
+10 mV
-10 mV
-50 mV
strep binding
5 nA
20 sec
strep *trans*
+50 mV
+10 mV
-10 mV
-50 mV
B
strep *trans*
0.1 nA
20 sec
strep *cis*
+60mV
+10mV
-10mV
-60mV
C
0.1 nA
1 min
strep binding
strep *trans*
voltage -10mV

sides of the membrane, and thus no site traverses membrane completely to the other side, extending out far enough so that the attached biotin could bind streptavidin. In two cases (S7C and T69C), streptavidin reduced the conductivity and gating of biotinylated channels both from the *cis* and *trans* sides of the membrane (shown for T69C in Fig. 8 *A*) in multichannel membranes. When these channels were observed in single-channel membranes, streptavidin was observed to act from either the *cis* or *trans* side, but not from both sides (Fig. 8 *B*). Thus, as with N38C, some biotinylated type 2 channel mutants are inserting in both of the two possible orientations. Nevertheless, each site does not become accessible to streptavidin on both sides of the membrane.

These results are summarized in Fig. 9. Only one conformation of the channel can bind streptavidin, resulting in trapping VDAC in one closed state. The chosen site is illustrated as traversing the membrane, consistent with previous observations that charges in this region influence the steepness of the voltage dependence. However, a site could easily be chosen that traverses only part of the membrane. In any case, to be consistent with the observations (prevent channel reopening and only bind in one closed conformation), the site must only be accessible to streptavidin in one conformation.

Alternative explanations of the type 2 effects are less likely because they either require a far more complex explanation or contradict previous experimental results. One could suggest that streptavidin is binding to static sites, rather than the mobile domain, but it blocks the gating process indirectly. If so, one would expect that sometimes the channels would be trapped open and sometimes trapped closed. This is not the case. All of the type 2 mutants were trapped in a low-conducting state consistent with the closed state, never in a full-conducting state. To account for this, one could further stipulate that in some cases the channels were trapped in the open state, but the conductance was reduced because of interference of ion flow by streptavidin. However, this hypothesis would have to somehow explain why the streptavidin-binding site becomes unavailable when the channel is closed with positive potentials on the streptavidin side. (Note that this is not the case for type 1 sites.) If the site is on a static region, it should not move when the channel gates. One might rationalize this by proposing that the site does not move, but is somehow covered during closure at positive potentials on the streptavidin side. Note that the protein cover would have to include not just the cysteine, but also the biotin and the long arm; this seems unlikely. Moreover, this cover would have to be generated when the positively charged sensor is being driven toward the opposite surface of the membrane (previous results support the existence of a positively charged sensor and the assumption that it moves in the field). Thus this alternative hypothesis would require that under conditions in which protein domains are being moved away from the streptavidin side, some hypothetical protein structure manages to cover each of the identified type 2 sites; this seems unlikely.

An additional argument in favor of our interpretation of the type 2 effects comes from the degree of conductance drop after streptavidin binding. The single-channel conductance drop for type 2 mutants is greater than for type 1, and this drop is very similar to that seen when channels are closed with an applied voltage. In Fig. 7 *B*, when streptavidin was added to a single channel held closed by voltage, there was no perceptible change in current flow upon streptavidin binding. That streptavidin had bound was evident when the voltage was reduced. This is different from what was seen when streptavidin was added to a single channel in the open state. There a clear, discrete conductance change was always seen. This is most simply explained if the streptavidin binding just holds the channel closed, rather than trapping the channel in the open state and interfering with gating and ion flow.

It must also be emphasized that for all type 2 sites, streptavidin acted when the streptavidin side was negative. Hypothetical sites that block closure in an indirect manner might be located in a variety of places and therefore might be affected under a variety of conditions, depending on the particular mutant. We conclude that the type 2 mutations identify sites in the molecule that are part of the voltage sensor, and that move from a site buried in the membrane to a site exposed at the surface of the membrane during channel closure.

When examined at the single-channel level, none of the biotinylated channels we examined was affected by streptavidin on both sides of the membrane. This means that the biotinylated residues that were exposed on one side of the membrane during one gating process never moved completely across the membrane to be exposed on the other side during the second gating process. This is in contrast to the results with colicin Ia, in which certain residues were found to be accessible to streptavidin on each side of the membrane, depending on the applied potential (Slatin et al., 1994). Although we have not tested every possible site in the VDAC molecule, these results suggest that movement of the sensor is restricted, such that it does not completely emerge from the membrane on either side.

FIGURE 7 Streptavidin traps VDAC channels, biotinylated at position 282, in the closed state only when added to the *trans* side. (*A*) As indicated, streptavidin was first added to the *cis* side and later to the *trans* side of a membrane containing multiple biotinylated E282C VDAC channels. The second addition was made after the channels had been closed by the application of −50 mV. The upper record is continuous with the lower record. (*B*) This is an experiment with a single biotinylated E282C channel. Streptavidin was first added to the *cis* side of the membrane without any effect. Streptavidin was then added to the *trans* side of the membrane after the channel was closed using +60 mV. (*C*) Streptavidin was added to the *trans* side of a membrane containing five E282C VDAC channels. The potential was held at −10 mV. Four of the five channels closed. At the end of the record, a new channel was inserted into the membrane. It was also trapped closed by the streptavidin. The voltage was kept constant at −10 mV.

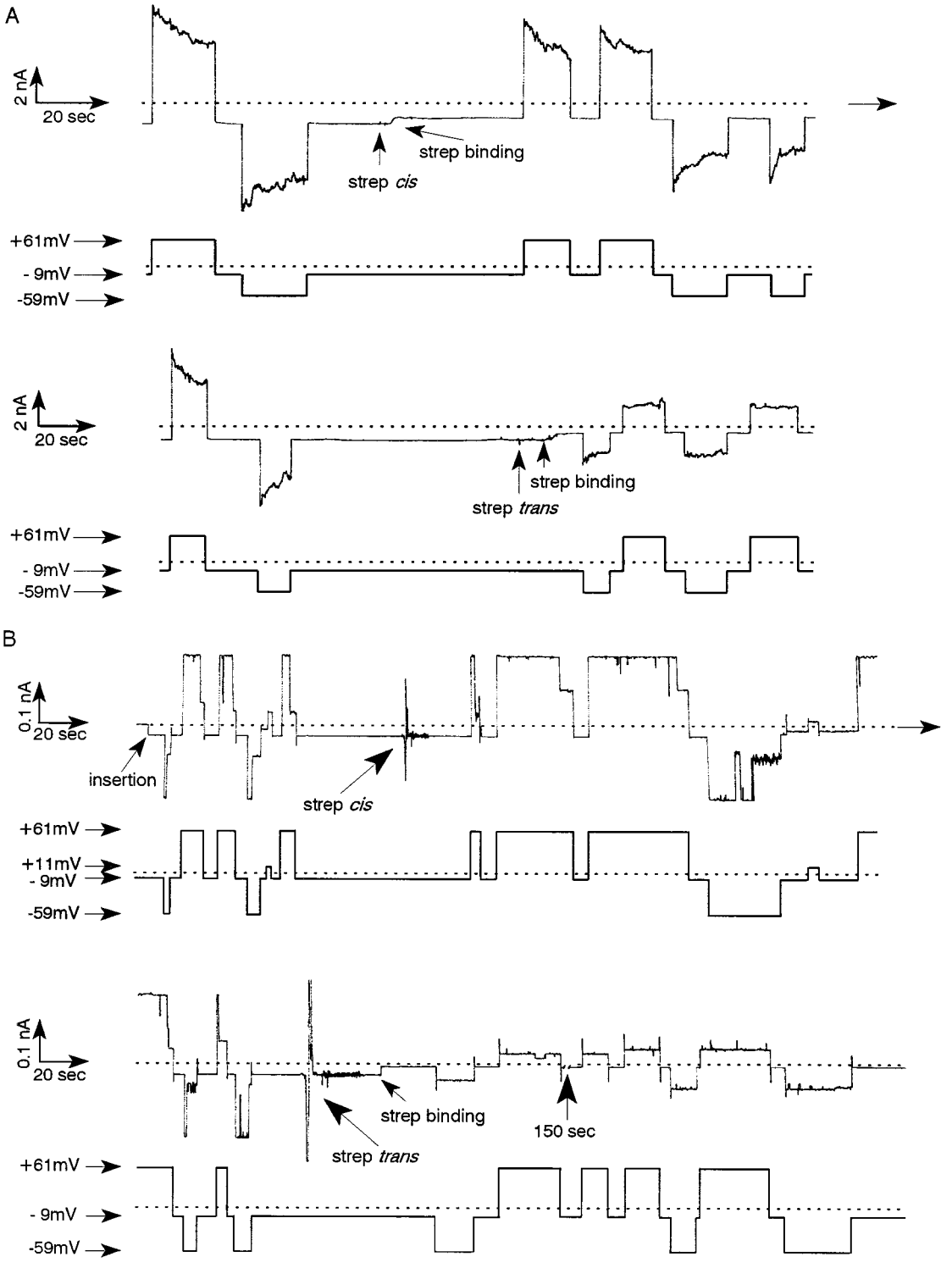

FIGURE 8 Streptavidin affected membranes containing multiple biotinylated T69C VDAC channels when added to either side, but single-channel membranes were only affected from one side. In *A*, a portion of the recorded current is illustrated in two segments, along with the associated voltage trace. There is no break in the time line. Streptavidin was first added to the *cis* side of this multichannel membrane. The current change, interpreted as streptavidin binding, is indicated. Streptavidin was subsequently added to the *trans* side. (*B*) This is a record of an experiment performed on a single channel. For clarity, a 150-s break in the time line was introduced where indicated. The points of channel insertion, streptavidin addition to the *cis* and *trans* sides, and streptavidin binding are indicated.

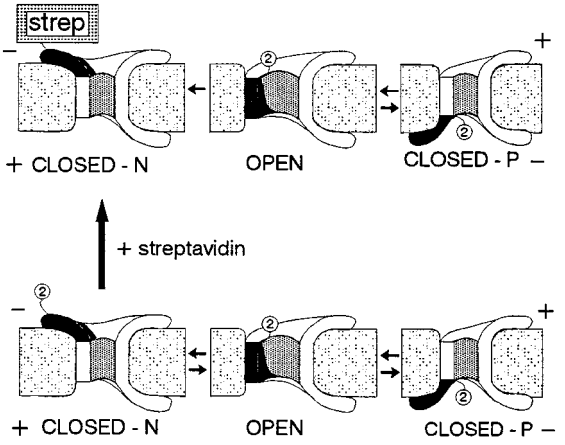

FIGURE 9 Mechanistic interpretation of the type 2 streptavidin effect. Type 2 sites are proposed to be on the sensor regions, and therefore are only accessible to streptavidin in the closed state when a negative potential is applied to the streptavidin side (CLOSED-N). The binding of streptavidin traps the channel in this closed state.

Type 2 sites are located on the voltage sensor

The location of type 2 mutations agrees well with previous results that localized the voltage sensor based on the effects of charge changes altering the gating properties of yeast VDAC (boxed residues in Fig. 1). The sites identified in this work in *N. crassa* VDAC (boxed residues in Fig. 10) are in the same regions—mainly in the first 80 or so amino acids and the very C-terminus, which would be adjacent to the N-terminus if the structure formed a cylinder. The agreement extends to the lack of motion in the first putative β-strand. Previous work identified site 30 (Fig. 1) as being in a static region, because charge changes at this site did not affect the steepness of the voltage dependence and did affect the closed-state selectivity. Here we identify nearby site 38 (Fig. 10) as a type 1 site, thus confirming a static region. Note that the first β-strand is flanked by mobile regions identified as such by previous and current experiments. Thus, although this stationary region in the middle of mobile regions is puzzling, the agreement is reassuring. Likewise, type 1 sites (*circled residues*), for which streptavidin binding reduces conductance but allows gating to occur, are located in the central portion of the molecule, in regions that generally agree with previous results that identified sites where charge changes did not alter the steepness of the voltage dependence (*circled residues* in Fig. 1).

The conformation of the VDAC protein in each of the closed states is undoubtedly very different. However, a largely common sensor domain is probably moving in both gating processes. Note, for example, that T53 and T69 are on opposite ends of a proposed transmembrane strand (Fig. 10). Streptavidin binding to either site locks the channel in a closed state. It seems most likely that those residues represent opposite ends of the mobile domain that can move out of the membrane in either direction, resulting in channel closure. Previous work showed that charge changes at many sites affected the steepness of the voltage dependence of both gating processes. At one site, position 46, this was

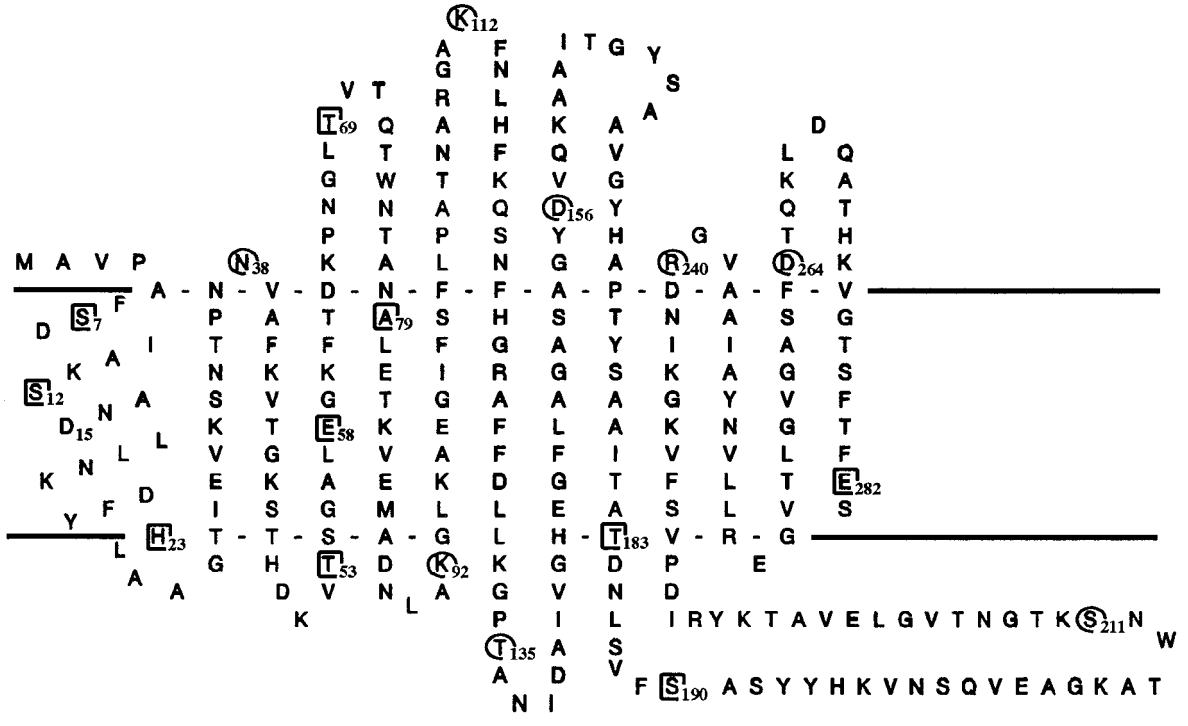

FIGURE 10 Transmembrane folding pattern showing the location of type 1 (*circled residues*) and type 2 (*squared residues*) mutations. This folding pattern for *N. crassa* VDAC was derived (Song and Colombini, 1996) in analogy to that developed for yeast (Blachly-Dyson et al., 1990). The lines show the boundary of the hydrophobic part of the membrane.

shown at the single-channel level. This is consistent with the observation that VDAC channels that have been closed by a potential of one polarity must enter the open state before closing in response to a potential of the opposite polarity (Colombini, 1986). It should be possible to distinguish between the sensor motion in two directions by creating VDAC molecules with biotin-modified residues at two separate positions and determining whether streptavidin affects these molecules from one or both sides of the membrane. Such experiments, now under way, should also reveal new information about the topology of the VDAC molecule in the membrane.

The current experiments monitor physical motion, whereas the previous experiments on the steepness of the voltage dependence detected motion of charge relative to the electric field. The electrical potential experienced by a charged residue on the protein can certainly change without physical motion of that charge. Therefore, a charged residue can influence the voltage dependence of the channel by experiencing a change in electrical potential without moving through the membrane. If so, determining whether a charge change at a site influences the steepness of the voltage dependence is not the same as measuring physical motion. The fact that the results of the two approaches agree so well demonstrates forcefully that we have identified the voltage sensor and that it moves through the membrane.

In this regard, there is a region in the middle of the central static portion where the two types of experiments seem to disagree. The 145–152 region has previously been proposed to slide up and down during both gating processes. This was concluded from a study of the effect of charge substitutions at sites 145 and 152 on the steepness of the voltage dependence (Zizi et al., 1995). E145K selectively increased the steepness of the voltage dependence of one gating process only, E152K increased that of the other, and the double mutant E145K/E152K increased the steepness of both. The simplest interpretation was a sliding strand. E145 moves through the electric field in one gating process and E152 in the other. However, the fact that D156C displayed type 1 behavior is puzzling, because binding of streptavidin to this sliding strand would be expected to interfere with the motion, especially motion away from streptavidin. Instead, as was the case for other type 1 mutations, motion toward streptavidin was interfered with. One possible interpretation may be that this strand is not physically moving. During the closing process, the conformational change of the channel changes the local electrical field felt by E152 and E145, and in this way the charge at these sites affects the steepness of the voltage dependence.

Another surprise was that S190 and T183 are found to be type 2 sites. Although the region around these sites had not been tested for its influence on the steepness of the voltage dependence, its location in the middle of an otherwise static central region of the molecule is unexpected. The presence of long nontransmembrane protein regions on either side of the 176–185 transmembrane strand may indicate that this strand is not located as illustrated in Fig. 10, but is actually located in the midst of a mobile region. If that were the case, the protein connections might serve to limit the motion of the mobile domain and perhaps develop some degree of tension that would be important in rapid reopening of the channel when the transmembrane voltage is reduced (as previously proposed; Colombini et al., 1996). Clearly, the molecular rearrangements associated with voltage gating are more complex than the simple movement of a contiguous domain of the protein from the interior of the membrane to the surface.

Estimation of the extent of protein biotinylation

Although an excess of biotinylating reagent was added to the VDAC-containing sample, the fraction of cysteines that reacted was variable. This probably reflected the degree of accessibility of a cysteine at the particular location in the molecule. The biotinylating reagent hydrolyzes in water, and so is only available to react for a short time. There is no evidence for different populations of channels with different levels of reactivity to the reagent. On the contrary, the degree of biotinylation can be increased by using a higher initial concentration of biotinylating reagent. The degree of biotinylation of the poorly biotinylated site, D15C, was increased from 32% to 69% by trebling the initial reagent concentration.

The extent of biotinylation of each cysteine substitution was assessed after SDS-polyacrylamide gel electrophoresis under conditions that allowed streptavidin-biotinylated VDAC complexes to survive electrophoresis. As shown in Fig. 11, unmodified or biotinylated protein in the absence of streptavidin has the molecular weight expected for the uncomplexed, VDAC protein. However, on the addition of streptavidin to biotinylated samples before electrophoresis, a slower-moving complex representing streptavidin-VDAC

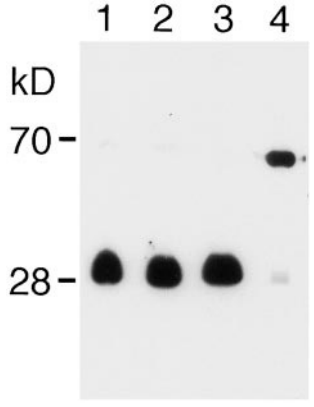

FIGURE 11 Western blot of an SDS polyacrylamide gel of VDAC-streptavidin complexes. Unbiotinylated (*lanes 1* and *2*) or biotinylated (*lanes 3* or *4*) VDAC mutant A79C were separated by SDS-polyacrylamide gel electrophoresis with (*lanes 2* or *4*) or without (*lanes 1* or *3*) the addition of streptavidin. The blot of the gel was visualized with anti-VDAC antibodies. The protein standards marked are 70 kDa and 28 kDa. The percentage of dimer formation is 0.2%, and the percentage of biotinylation is 92.2%.

complexes was clearly separated from uncomplexed VDAC. Image analysis of the amount of VDAC in each band provides the estimate of the extent of biotinylation of each mutant; this is shown in Table 3 (column 2, % biotinylation).

A functional assay for the extent of biotinylation was also used. Here, the percentage of the channels reconstituted in the planar membrane that could respond to streptavidin was assessed (Materials and Methods; Table 3, column 1). The percentage of channels affected by streptavidin agrees quite well at most sites with the percentage biotinylation determined by the gel assay. The differences (column 3, the discrepancy) could arise from biased insertion of either unbiotinylated or biotinylated channels, or from inaccessibility of at least some of the tethered biotin to the added streptavidin.

The sites with the highest discrepancy are D15, E58, and E282. Although hundreds of D15C channels were tested, no channels were ever observed to be affected by streptavidin, despite the fact that the majority of channels have been biotinylated, as assessed by the gel assay. Inaccessibility seems to be the likely explanation for the inability to observe an effect of streptavidin binding on VDAC biotinylated at position 15. Because charge changes at this position were shown to influence ion selectivity in open channels, but not in closed channels, and they altered the steepness of the voltage dependence (Peng et al., 1992b; Thomas et al., 1993), this position should face the ion stream in the open state and move through the field and away from the ion stream during the closing process. The lack of effect of streptavidin probably indicates that streptavidin is not binding to any VDAC conformation. If so, a likely conclusion is that D15 is in the middle of the channel and moves to one surface upon channel closure, but not far enough to be accessible to streptavidin. Streptavidin is basically a 5.5-nm cube, and its surface must get within 0.7 nm of the sulfur on the cysteine for tight binding to biotin to occur (because of the length of biotin's molecular tether and the depth of the binding site on streptavidin). Thus steric factors could prevent binding to sites even close to or at the surface. Exposed domains may have a structure that prevents access of streptavidin to biotinylated residues after movement of these domains from sites within the bilayer to the surface during channel closure. The alternative explanation that only unbiotinylated channels are inserting seems unlikely, because that is not the case for nearby positions, such as 7, 12, and 23. The poor level of protein biotinylation at position 15, even when three times the normal amount of reagent was used, indicates that D15 is poorly accessible. This is consistent with a location in the middle of the channel, perhaps forming a salt bridge with a neighboring lysine residue.

TABLE 3 Comparison of the percentage of reconstituted channels affected by streptavidin and the percentage of proteins biotinylated according to Western blotting assay

Mutant	% affected	% biotinylated	Discrepancy	Preference
S7C	33	59	−26	3
S12C	61	48	13	0.6
D15C*	<2	68	>−66	>104[#]
H23C	82	96	−14	5
N38C	90	98	−8	5
T53C	79	77	2	0.9
E58C	27	90	−63	24[#]
T69C	89	95	−6	2
A79C	80	92	−12	3
K92C	43	49	−6	1
K112C	63	91	−28	6
T135C	80	86	−6	2
D156C	58	35	23	0.4
T183	39	80	−41	6
S190C	80	89	−9	2
R240C	83	92	−9	2
D264C	79	79	0	1
E282C	44	89	−45	10[#]
GGC extension	65	81	−16	2

The discrepancy is % biotinylated − % affected. The preference is (% biotinylated − % unaffected)/(% unbiotinylated − % affected) and is the fold preference for insertion of unbiotinylated channels.

*The concentration of 3-(-*N*-maleimidylpropionyl)biocytin used to biotinylate this mutant was 9 mg/ml, instead of 3 mg/ml, to increase the degree of biotinylation.

[#]Greater than 10-fold preference.

The discrepancy for positions 58 and 282 likely results from biased insertion in favor of unbiotinylated channels. Because many channels did bind streptavidin, streptavidin was in excess, and the changes induced by streptavidin in a multichannel membrane occurred over a relatively short period of time, poor accessibility seems an invalid conclusion. It also seems unlikely that there was a subpopulation of biotinylated channels in a conformation where these sites were inaccessible to streptavidin, because we went through many voltage-induced opening and closing cycles in the presence of streptavidin without further significant effect. Assuming that biased insertion underlies the discrepancy, one can estimate the fold preference for insertion of unbiotinylated channels (column 4). For positions 58 and 282, there would have to be a greater than 10-fold preference for insertion of unbiotinylated channels to account for the observations.

Localization of sites at the rim of the channel

The degree of channel obstruction after streptavidin binding can yield information on how close the cysteine (to which the streptavidin is tethered) is to the channel opening. Streptavidin binding to the channels containing the type 1 mutation results in a reduction of the conductance of the channel, which we interpret as a physical occlusion of part of the channel opening. The amount of reduction in conductance can be used as a measure of the extent of occlusion and be related to the location of the site to which the streptavidin is attached.

The required structural information for the calculations is available. The binding pockets for biotin on streptavidin are deep. From the known crystal structure of streptavidin and

from the length of the molecular arm connecting the cysteine to the biotin moiety, one can determine that a 0.7-nm molecular linker connects the sulfur of the cysteine to the streptavidin surface, whose relative rigidity allows for an estimated 0.5 nm in lateral motion. The molecular footprint (Fig. 12) for streptavidin was obtained from published electron microscopical analyses of arrays of streptavidin attached to biotinylated phospholipid monolayers (Avila-Sakar and Chiu, 1996). The amount of occlusion of the 3-nm pore was calculated by assuming that the streptavidin could move randomly and was only restricted by its attachment to VDAC through the molecular linker. The average fractional unobstructed pore area of 10,000 random streptavidin orientations (random values of angles α and δ in Fig. 12) was determined as a function of distance of the attachment site on VDAC (the cysteine sulfur) from the edge of the pore (t-pore radius in Fig. 12). This was used to generate the solid line in the figure. This theoretical line was used to convert the fractional conductance remaining after streptavidin binding to single channels with type 1 substitutions (tabular data in Fig. 13) to distances from the rim of the pore (*triangles* in Fig. 12). The results are shown diagrammatically in Fig. 13. In the figure, the protein wall is taken as a cylinder, using the diameter from Mannella's measurements of frozen/hydrated samples (Mannella et al., 1989). The thickness on each side of the wall is the average amino acid side-chain length of 0.5 nm. The calculated distances were applied as outward from the inner circle. The location along the circumference was taken from our current folding pattern for the protein in the membrane. The effective distance between β-strands is longer than expected, because of an unknown amount of strand tilt in the protein.

This top-view projection shows the location of the type 1 sites around the rim of the pore. The contribution made by this analysis is an estimate of the distance of the sites from the inner edge of the wall of the pore. When combined with the identified transmembrane strands and the known structure of β-barrels, one can obtain an idealized picture of the surface structure of the channel. This is structural informa-

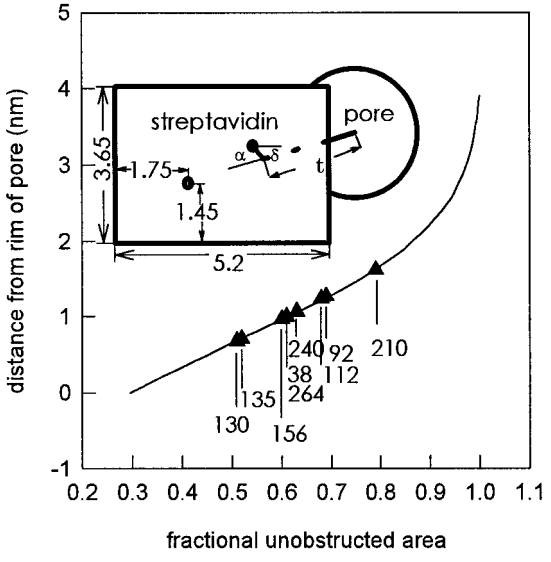

FIGURE 12 Calculation of the degree of occlusion of the pore by streptavidin binding to type 1 sites. The drawing within the figure shows the opening of the channel (*circle*, 3 nm in diameter) and the streptavidin contact region, or footprint, approximated as a rectangle (5.2 × 3.65 nm). Two biotin binding sites that would face the membrane surface are shown as small circles 1.75 and 1.45 nm away from the edge of the footprint. A short, thick line, representing the molecular linker of the biotinylating reagent, connects one of these sites to the cysteine sulfur on VDAC. The angles α and δ that were varied to randomly change the orientation of streptavidin are defined as indicated in Materials and Methods. The calculated distance from the site of streptavidin attachment on VDAC to the rim of the pore (t-pore radius) is plotted against the averaged fractional unobstructed area of the pore (*solid curve*). The fractional unobstructed area was calculated by assuming that streptavidin could take all possible orientations and for values of t ranging from 1.5 nm (located at the rim), to the point where no obstruction occurred at 0.1-nm intervals. The fraction of conductance remaining after streptavidin binding to the type 1 mutant channels was equated to the fractional unobstructed area and plotted on the theoretical curve (*triangles*). The locations on the protein sequence are indicated.

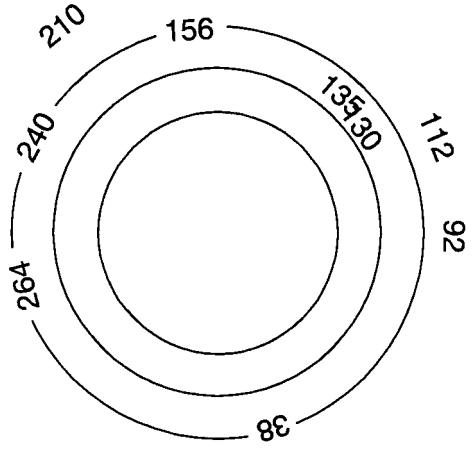

Position	Fractional G	distance (nm)
38	0.61	0.99
92	0.69	1.27
112	0.68	1.23
130	0.51	0.65
135	0.52	0.69
156	0.6	0.95
210	0.79	1.63
240	0.63	1.06
264	0.61	0.99

FIGURE 13 An end-view projection of a current model of the VDAC channel, showing the location of the type 1 sites around the rim of the pore. The theoretical line in Fig. 4 was used to convert the fractional conductance remaining after streptavidin binding to single channels with type 1 substitutions to distances of each site from the rim of the pore (tabular data). The inner middle and outer circles represent the inner boundary of the channel where the amino acid side chains projecting into the pore end, the location of the protein backbone, and the outer perimeter of the channel proper (excluding extended surface domains), respectively. The calculated distances were applied as outward from the inner circle. The location along the circumference was taken from our current folding pattern for the protein in the membrane. The effective distance between β-strands is longer than expected, because of an unknown amount of strand tilt in the protein.

tion that so far has been unavailable by any other means. It must be regarded with some caution, because we assumed that streptavidin took all possible orientations and disregarded any leakage of ions between the VDAC surface and the streptavidin surface. In any case, the reasonableness of the results of these calculations with no free parameters provides strong confirmation of the mechanism by which the conductance is reduced when streptavidin binds to type 1 sites. It also argues for a surface topography for the channel that is rather flat and does not protrude much into the aqueous phase. This is consistent with the low-resolution surface topography of VDAC obtained by electron microscopy of freeze-dried two-dimensional crystals (Thomas et al., 1991), and quite different from channels such as the acetylcholine receptor.

Biotinylation biases the insertion direction

Our results do not tell us whether VDAC channels biotinylated at different sites insert into the bilayer in the same orientation, and thus we cannot distinguish which of the two gating processes is being affected by streptavidin binding at a particular site. In addition, we do not know why channels that are biotinylated at some sites insert preferentially in one orientation, whereas those biotinylated at other sites insert in both orientations. Yeast VDAC has been shown to insert into the membrane in both directions (Zizi et al., 1995), and our results suggest that biotinylation biases the insertion direction. Biotinylation may also interfere with the previously described autodirected insertion process (Zizi et al., 1995).

In summary, we have found that VDAC channels that have been biotinylated at a single introduced cysteine residue and inserted into planar phospholipid membranes can be affected by streptavidin addition in one of two different ways. The characteristics of each site are those predicted for residues that either do not move during voltage gating (type 1), or residues that move from locations within the bilayer in the open channel to sites that are exposed at the membrane surface during channel closure (type 2). By combining the biotin-streptavidin technology with site-directed mutations and the electrophysiology of reconstituted channels, we have provided direct evidence for the motion of the VDAC sensor regions through the membrane during the gating process. Our results agree well with previous data, but add new insight in terms of the sensor domains and the extent of their motion.

We thank Carmen Mannella for the gift of the antibody and Denny Gulick and Thanhlong Nguyen for help with the pore occlusion calculations.

The research was supported by the National Institutes of Health (GM 35759).

REFERENCES

Avila-Sakar, A. J., and W. Chiu. 1996. Visualization of β-sheets and side-chain clusters in two-dimensional periodic arrays of streptavidin on phospholipid monolayers by electron crystallography. *Biophys. J.* 70: 57–68.

Benz, R., L. Wojtczak, W. Bosch, and D. Brdiczka. 1988. Inhibition of adenine nucleotide transport through the mitochondrial porin by a synthetic polyanion. *FEBS Lett.* 231:75–80.

Blachly-Dyson, E., S. Peng, M. Colombini, and M. Forte. 1990. Selectivity changes in site-directed mutants of the VDAC ion channel: structural implications. *Science.* 247:1233–1236.

Blachly-Dyson, E., J. M. Song, W. J. Wolfgang, M. Colombini, and M. Forte. 1997. Multicopy suppressors of phenotypes resulting from the absence of yeast VDAC encode a VDAC-like protein. *Mol. Cell. Biol.* 17:5727–5738.

Bowen, K. A., K. Tam, and M. Colombini. 1985. Evidence for titratable gating charges controlling the voltage dependence of the outer mitochondrial membrane channel, VDAC. *J. Membr. Biol.* 86:51–59.

Colombini, M. 1986. Voltage Gating in VDAC. Toward a Molecular Mechanism. *In* Ion Channel Reconstitution. C. Miller, editor. Plenum Press, New York. 533–550.

Colombini, M. 1987. Characterization of channels isolated from plant mitochondria. *Methods Enzymol.* 148:465–475.

Colombini, M. 1989. Voltage gating in the mitochondrial channel, VDAC. *J. Membr. Biol.* 111:103–111.

Colombini, M., E. Blachly-Dyson, and M. Forte. 1996. VDAC, a channel in the outer mitochondrial membrane. *In* Ion Channels, Vol. 4. T. Narahashi, editor. Plenum Press, New York. 169–202.

Doring, C., and M. Colombini. 1985. Voltage dependence and ion selectivity of the mitochondrial channel, VDAC, are modified by succinic anhydride. *J. Membr. Biol.* 83:81–86.

Larsson, H. P., O. S. Baker, D. S. Dhillon, and E. Y. Isacoff. 1966. Transmembrane movement of the Shaker K^+ channel S4. *Neuron.* 16:387–397.

Lee, A.-C., M. Zizi, and M. Colombini. 1994. β-NADH decreases the permeability of the mitochondrial outer membrane to ADP by a factor of 6. *J. Biol. Chem.* 269:30974–30980.

Liu, M., and M. Colombini. 1992. Regulation of mitochondrial respiration by controlling the permeability of the outer membrane through the mitochondrial channel VDAC. *Biochim. Biophys. Acta.* 1098:255–260.

Mannella, C. A. 1989. Structure of the mitochondrial outer membrane channel derived from electron microscopy of 2D crystals. *J. Bioenerg. Biomembr.* 21:427–437.

Mannella, C. A., and M. Colombini. 1984. Evidence that the crystalline arrays in the outer membrane of *Neurospora* mitochondria are composed of the voltage-dependent channel protein. *Biochim. Biophys. Acta.* 774: 206–214.

Mannella, C. A., X. W. Guo, and B. Cognon. 1989. Diameter of the mitochondrial outer membrane channel: evidence from electron microscopy of frozen-hydrated membrane crystals. *FEBS Lett.* 253:231–234.

Montal, M., and P. Mueller. 1972. Formation of bimolecular membranes from lipid monolayers and a study of their electrical properties. *Proc. Natl. Acad. Sci. USA.* 69:3561–3566.

Peng, S., E. Blachly-Dyson, M. Forte, and M. Colombini. 1992a. Determination of the number of polypeptide subunits in a functional VDAC channel from *Saccharomyces cerevisiae*. *J. Bioenerg. Biomembr.* 24: 27–31.

Peng, S., E. Blachly-Dyson, M. Forte, and M. Colombini. 1992b. Large scale rearrangement of protein domains is associated with voltage gating of the VDAC channel. *Biophys. J.* 62:123–135.

Qiu, X. Q., K. S. Jakes, A. Finkelstein, and S. L. Slatin. 1994. Site-specific biotinylation of colicin Ia. *J. Biol. Chem.* 269:7483–7488.

Rostovtseva T., and M. Colombini. 1997. VDAC channels mediate and gate the flow of ATP: implications for the regulation of mitochondrial function. *Biophys. J.* 72:1954–1962.

Seoh, S. A., D. Sigg, D. M. Papazian, and F. Bezanilla. 1996. Voltage-sensing residues in the S2 and S4 segments of the Shaker K^+ channels. *Neuron.* 16:1159–1167.

Slatin, S. L., X. Q. Qiu, K. S. Jakes, and A. Finkelstein. 1994. Identification of a translocated protein segment in a voltage-dependent channel. *Nature.* 371:158–161.

Song, J., and M. Colombini. 1996. Indications of a common folding pattern for VDAC channels from all sources. *J. Bioenerg. Biomembr.* 28: 153–161.

Stanley, S., J. Dias, D. D'Arcangelis, and C. Mannella. 1995. Peptide-specific antibodies as probes of the topography of the voltage-gated channel in the mitochondrial outer membrane of *Neurospora crassa*. *J. Biol. Chem.* 270:16694–16700.

Thomas, L., E. Blachly-Dyson, M. Colombini, and M. Forte. 1993. Mapping of residues forming the voltage sensor of the VDAC channel. *Proc. Natl. Acad. Sci. USA.* 90:5446–5449.

Weber, P. C., D. H. Ohlendorf, J. J. Wendoloski, and F. R. Salemme. 1989. Structural origins of high-affinity biotin binding to streptavidin. *Science.* 243:85–88.

Yang, N., A. L. George, Jr., and R. Horn. 1996. Molecular basis of charge movement in voltage-gated sodium channels. *Neuron.* 16:113–122.

Zizi, M., M. Forte, E. Blachly-Dyson, and M. Colombini. 1994. NADH regulates the gating of VDAC, the mitochondrial outer membrane channel. *J. Biol. Chem.* 269:1614–1616.

Zizi, M., L. Thomas, E. Blachly-Dyson, M. Forte, and M. Colombini. 1995. Oriented channel insertion reveals the motion of a transmembrane beta strand during voltage gating of VDAC. *J. Membr. Biol.* 144: 121–129.